A PLATE BENDING FINITE ELEMENT MODEL WITH A LIMIT ANALYSIS CAPACITY

W. C. McCarthy
L. A. Traina

Department of Civil Engineering, New Mexico State University,
Las Cruces, New Mexico

Abstract. A knowledge of the reserve strength of plates will result in more economical designs, practical load capacity limits, and retrofit decisions that increase the strength of a structure. However, plates do not readily lend themselves to an elasto-plastic solution. One plate model, the grid framework, is the exception. The grid framework finite element models a plate through the use of grid members with a proven elasto-plastic analytical capability. The finite element mechanics of the grid-framework model are outlined with emphasis on the derivation process to generate the equivalent properties that force the grid-framework to conform to plate behavior. The concept of a limit analysis is introduced with a discussion of the elasto-plastic conversion procedure. An elasto-plastic solution to a plate structure is used to confirm the equivalent grid technique.

Keywords. Computer programming; finite automata; limit cycles; matrix algebra; modelling; elasto-plastic.

INTRODUCTION

Elasto-plastic analysis of plates is a complex affair using standard finite elements. One or the other of two alternatives is typically used. In the first approach, the element is treated as an elastic continuum with its properties appropriately adjusted to yield levels to produce plastic action. This approach, although technically simple, requires a large number of elements to adequately define yield patterns. The second alternative is to establish the element as an elasto-plastic medium that simultaneously exhibits both elastic and plastic behavior thus, reducing the need for a large system. To produce this combination, however, requires a highly complicated mathematical formulation.

The dilemma of complicated development versus a large system is resolved with a nonstandard alternative in the form of an equivalent grid or grid framework element first proposed by Yettram and Husain (1965) and later expanded by Traina (1968). The grid-framework element uses six grid members interconnected at four corners to model a plate element. This arrangement has several advantages over plate elements including faster convergence in many instances, multiple yield directions and potential yield points, and the ability to readily interface with plane grid structures. In addition, the grid framework element lends itself to a limit analysis and, in this capacity, a previously defined (McCarthy, White, and Minor, 1980) matrix modification process that introduces plasticity to grid structures. The grid framework limit analysis, developed through the Engineering Foundation (McCarthy, 1982) follows a cyclical analysis procedure described by Wang (1970) where "hinges" are inserted into a structure to simulate yielding.

MATRIX FORMULATION

Plate behavior is simulated by the grid-framework element only when the grid member properties are suitably determined by establishing moment equilibrium and modal compatibility between the equivalent grid and a plate element. Equilibrium and compatibility requires the use of the grid-framework stiffness matrix with the skewed grid framework element of Fig. 1 as the starting point in this matrix development. A single grid member has two bending moments and a torsional moment representing internal forces {F} and their corresponding displacements {e}. External forces {P} and displacements {X} associated with an element act at the four corners referred to as nodes or joints. Figure 2 illustrates the internal and external force layout. Static equilibrium between the external and internal forces at the four nodes produces a statics matrix [A] and the matrix equation

$$\{P\} = [A]\{F\} \qquad (1)$$

For a typical member of the grid-framework element, defined by end nodes i and j, slope deflection and elastic torsion results in

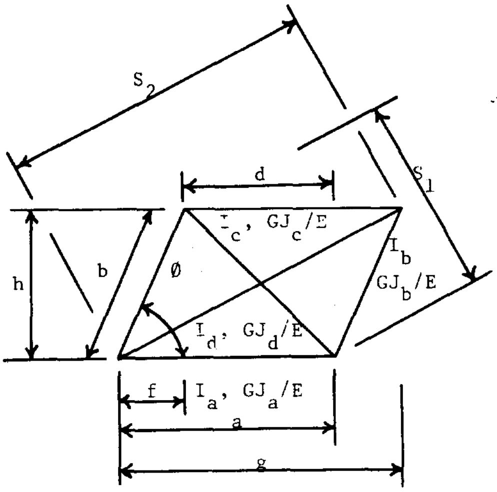

where: Ø = skew angle d = a − f
h = bsinØ g = a + f
f = bcosØ

$$s_1 = \sqrt{a^2 - 2ab\cos\emptyset + b^2}$$

$$s_2 = \sqrt{a^2 + 2ab\cos\emptyset + b^2}$$

Fig. 1. Skewed grid-framework model.

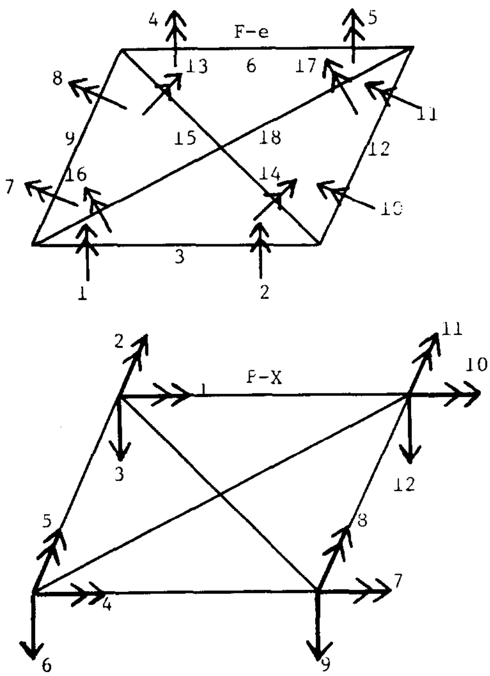

Fig. 2. Internal and external forces and displacements.

Equation 2 where e_k represents torsional rotation and EI and GJ are the flexural and

$$F_i = \frac{4EI}{L} e_i + \frac{2EI}{L} e_j$$

$$F_j = \frac{2EI}{L} e_i + \frac{4EI}{L} e_j \qquad (2)$$

$$F_k = \frac{GJ}{L} e_k$$

torsional stiffness, respectively. Equation 2, when applied to the six grid members, generates the member stiffness matrix ⌊S⌋ and the matrix equation

$$\{F\} = \lfloor S \rfloor \{e\} \qquad (3)$$

Now, conservation of energy or $X^T P = {}^T F$ combines with equations 1 and 3 to obtain the key equation

$$\{P\} = \lfloor A \rfloor \lfloor S \rfloor \lfloor A \rfloor^T \{X\} = \lfloor ASA^T \rfloor \{X\} \qquad (4)$$

where $\lfloor ASA^T \rfloor$ is the grid-framework stiffness matrix of Table 1 (tables at end of text).

Once the grid properties are known, a plate is analyzed due to external forces {P} and by solving Equation 4 for displacements {X}. Further manipulation of Equation 3 and the conservation of energy produces the second key equation

$$\{F\} = \lfloor S \rfloor \lfloor A \rfloor^T \{X\} = \lfloor SA^T \rfloor \{X\} \qquad (5)$$

Thus, the internal forces are found through the substitution of {X} from Equation 4 into Equation 5.

PLATE RELATIONSHIPS

A standard rectangular plate element is acted upon by bending moments M_x and M_y and a a twisting moment M_{xy} along the edges. These moments are distributed to the adjoining nodes as shown in Fig. 3.

The plate displacements are a function of the modulus of elasticity, E, Poisson's ratio, μ, and moment of inertia per unit width, $I = t^3/12$, where t is the plate thickness. The bending moments, taking into account the Poisson effect, cause rotations which may be determined by applying moment-area to the M/EI diagrams of Fig. 4. The twisting moment causes both rotations and displacements normal to the plane. The generalized forces and displacements at the corner nodes due to M_x, M_y and M_{xy} are summarized in Table 2.

GRID PROPERTIES

Working with the plate relationships of Table 2 and the grid-framework stiffness matrix of Table 1 and Equation 4, the correct grid properties may be found. The moments in Table 2 are substituted into the left hand side of Equation 4 for {P} while the displacements are substituted for {X}. This creates thirty six equations which, through replication, are reduced to the following twelve.

$$0 = -\mu EI_a + \left[\frac{ht^2}{b^2} - \frac{3\mu at^2}{b^3}\right]EI_b + \left[\frac{-ht}{b^2}\right]GJ_b + \left[\frac{ghb}{s_2^3} - \frac{\mu ag^2}{s_2^3}\right]EI_d - \left[\frac{ghb}{s_2^3} + \frac{\mu ah^2}{s_2^3}\right]GJ_d \qquad (6)$$

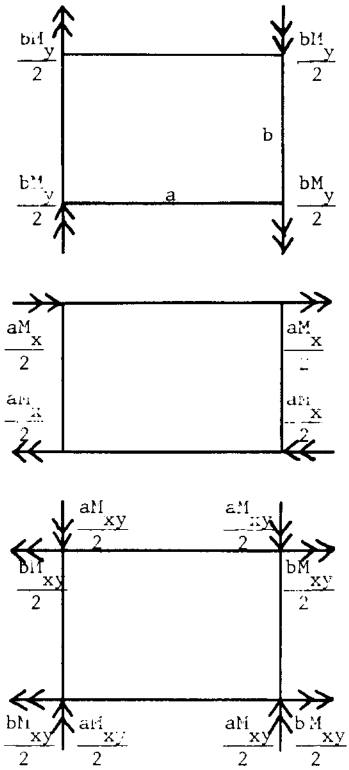

Fig. 3. Forces at the nodes-plate element.

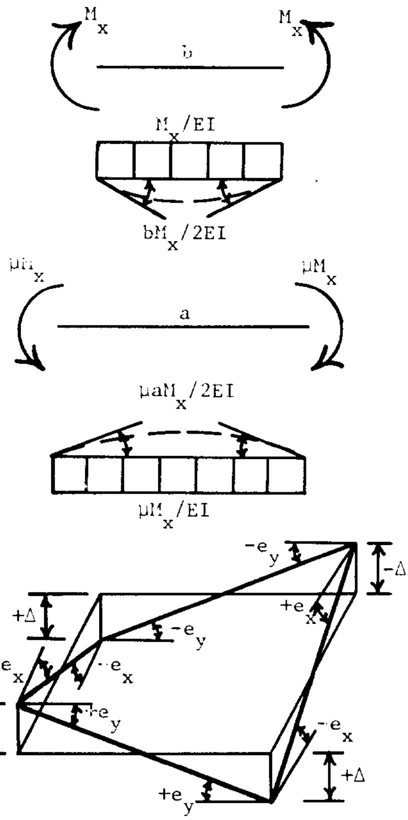

$$\Delta = \frac{M_{xy}(1+\mu)ab}{4EI} \qquad e_x = \frac{2\Delta}{b} \qquad e_y = \frac{2\Delta}{a}$$

Fig. 4. Rotations and displacements-plate element.

$$0 = \left[-\frac{\mu h^2}{b^2} + \frac{3fha}{b^3}\right]EI_b - \left[\frac{\mu f^2}{b^2}\right]GJ_b + \left[\frac{gha}{s_2^{\,3}} - \frac{\mu bh^2}{s_2^{\,3}}\right]EI_d - \left[\frac{hga}{s_2^{\,3}} + \frac{\mu bg^3}{s_2^{\,3}}\right]GJ_d \tag{7}$$

$$0 = -\mu EI_a - \left[\frac{hf}{b^2} + \frac{3\mu af^2}{b^3}\right]EI_b + \left[\frac{fh}{b^2}\right]GJ_b + \left[\frac{hdb}{s_1^{\,3}} - \frac{\mu ad^2}{s_1^{\,3}}\right]EI_c - \left[\frac{dhb}{s_1^{\,3}} - \frac{\mu ah^2}{s_1^{\,3}}\right]GJ_c \tag{8}$$

$$0 = \left[\frac{\mu h^2}{b^2} - \frac{3fha}{b^3}\right]EI_b - \left[\frac{\mu f^2}{b^3}\right]GJ_b + \left[\frac{hda}{s_1^{\,3}} - \frac{\mu bh^2}{s_1^{\,3}}\right]EI_c - \left[\frac{adh}{s_1^{\,3}} + \frac{\mu bd^2}{s_1^{\,3}}\right]GJ_c \tag{9}$$

$$\frac{EIa}{2} = \left[\frac{h^2}{b^2} + \frac{3\mu afh}{b^3}\right]EI_b + \left[\frac{f^2}{b^2}\right]GJ_b + \left[\frac{bh^2}{s_1^{\,3}} - \frac{\mu ahd}{s_1^{\,3}}\right]EI_c + \left[\frac{bd^2}{s_1^{\,3}} + \frac{\mu adh}{s_1^{\,3}}\right]GJ_c \tag{10}$$

$$\frac{EIb}{2} = EI_a + \left[\frac{\mu hf}{b^2} + \frac{3af^2}{b^3}\right]EI_b + \left[\frac{-\mu hf}{b^2}\right]GJ_b + \left[\frac{ad^2}{s_1^{\,3}} - \frac{\mu bdh}{s_1^{\,3}}\right]EI_c + \left[\frac{ah^2}{s_1^{\,3}} + \frac{\mu bdh}{s_1^{\,3}}\right]GJ_c \tag{11}$$

$$\frac{EIa}{2} = \left[\frac{h^2}{b^2} - \frac{3\mu afh}{b^3}\right]EI_b + \left[\frac{f^2}{b^2}\right]GJ_b + \left[\frac{bh^2}{s_2^{\,3}} - \frac{\mu agh}{s_2^{\,3}}\right]EI_d + \left[\frac{bg^2}{s_2^{\,3}} + \frac{\mu agh}{s_2^{\,3}}\right]GJ_d \tag{12}$$

$$\frac{EIb}{2} = EI_a + \left[\frac{-\mu hf}{b^2} + \frac{3af^2}{b^3}\right]EI_b + \left[\frac{\mu hf}{b^2}\right]GJ_b + \left[\frac{ag^2}{s_2^{\,3}} - \frac{\mu bgh}{s_2^{\,3}}\right]EI_d + \left[\frac{ah^2}{s_2^{\,3}} + \frac{\mu bhg}{s_2^{\,3}}\right]GJ_d \tag{13}$$

$$\frac{EIa}{2(1+\mu)} = \left[\frac{-3hfa}{b^3} + \frac{f^2}{b^2} + \frac{3fa}{b^2}\right]EI_b + \left[\frac{fh}{b^2}\right]GJ_b + \left[\frac{hda}{s_1^{\,3}} + \frac{bd^2}{s_1^{\,3}}\right]EI_c + \left[\frac{-hda}{s_1^{\,3}} + \frac{bh^2}{s_1^{\,3}}\right]GJ_c \tag{14}$$

$$\frac{EIb}{(1+\mu)} = GJ_a + \left[\frac{3ah^2}{b^3} - \frac{fh}{b^2} - \frac{3ah}{b^2}\right]EI_b + \left[\frac{fh}{b^2}\right]GJ_b + \left[\frac{ah^2}{s_1^{\,3}} + \frac{hdb}{s_1^{\,3}}\right]EI_c + \left[\frac{ad^2}{s_1^{\,3}} - \frac{hdb}{s_1^{\,3}}\right]GJ_c \tag{15}$$

$$\frac{EIb}{2(1+\mu)} = GJ_a + \left[\frac{3ah^2}{b^3} + \frac{fh}{b^2} - \frac{3ah}{b^2}\right]EI_b - \left[\frac{fh}{b^2}\right]GJ_b + \left[\frac{ah^2}{s_2^{\,3}} + \frac{hgb}{s_2^{\,3}}\right]EI_d + \left[\frac{ag^2}{s_2^{\,3}} - \frac{hgb}{s_2^{\,3}}\right]GJd \tag{16}$$

$$\frac{EIa}{2(1+\mu)} = \left[\frac{3hfa}{b^3} + \frac{f^2}{b^2} - \frac{3fa}{b^2}\right]EI_b + \left[\frac{h^2}{b^2}\right]GJ_b + \left[\frac{hga}{s_2^{\,3}} + \frac{bg^2}{s_2^{\,3}}\right]EI_d + \left[\frac{-hga}{s_2^{\,3}} + \frac{bh^2}{s_2^{\,3}}\right]GJ_d \tag{17}$$

Now, by assuming that $J_d = J_c = 0$ as proposed by Yettram and Husain (1965), Equations (6) through (17) are solved for the remaining properties to get:

$$I_c = \frac{2\mu S[V + \mu L]}{(1 - \mu^2)[MV + \mu ML + XR + \mu PX]} \qquad (18)$$

$$I_d = \frac{2\mu S[V + \mu L]}{(1 - \mu^2)[MV + \mu ML + XR + \mu PX]} \qquad (19)$$

$$I_b = \frac{AS - \left(\frac{CS}{1+\mu}\right) - [AD-\mu AX-CF-CX]\, I_c}{[A^2 + \mu AB + BC - C^2 - CH]} \qquad (20)$$

$$\frac{GJ_b}{E} \quad \frac{S}{A(1+\mu)} + \left[\left(\frac{B-C-H}{A}\right) I_b\right] - \left[\frac{F+X}{A}\right] I_c \qquad (21)$$

$$I_a = T - [HU + \mu W]\, I_b + \frac{\mu WGJ_b}{E} - [V-\mu K]\, I_c \qquad (22)$$

$$\frac{GJ_a}{E} = \frac{T}{(1+\mu)} + [W+Z-Y]\, I_b - \frac{WGJ_b}{E} - [L+K]\, I_c \qquad (23)$$

where

$$A = \frac{h^2}{b^2} \quad B = \frac{3afh}{b^3} \quad C = \frac{t^2}{b^2} \quad D = \frac{bh^2}{s_1^3}$$

$$F = \frac{bd^2}{s_1^3} \quad H = \frac{3at}{b^2} \quad K = \frac{bdh}{s_1^3} \quad L = \frac{ah^2}{s_1^3}$$

$$M = \frac{agh}{s_2^3} \quad P = \frac{ah^2}{s_2^3} \quad R = \frac{ag^2}{s_2^3} \quad S = \frac{at}{2}$$

$$T = \frac{bt}{2} \quad U = \frac{t}{b} \quad V = \frac{ad^2}{s_1^3} \quad W = \frac{ht}{b^2}$$

$$X = \frac{ahd}{s_1^3} \quad Y = \frac{3ah^2}{b^3} \quad Z = \frac{3ah}{b^2}$$

Further, for a right grid where $s = s_1 = s_2$, $I_c = I_d$, and $J_c = J_d$, Equations (6) to (17) are reduced to six equations which produce the Traina solution as follows:

$$I_a = \frac{(b^2 - \mu a^2)I}{2b(1-\mu^2)} - \left[\frac{ab^2 + a^3}{s^3}\right]\frac{GJ_d}{E}$$

$$I_b = \frac{(a^2 - \mu b^2)I}{2a(1-\mu^2)} + \left[\frac{b^3 + a^2 b}{s^3}\right]\frac{GJ_d}{E}$$

$$I_d = \frac{s^3 \mu I}{2ab(1-\mu^2)} + \frac{GJ_d}{E}$$

$$\frac{GJ_a}{E} = \frac{b(1-3\mu)I}{2(1-\mu^2)} - \left[\frac{ab^2+a^3}{s^3}\right]\frac{GJ_d}{E}$$

$$\frac{GJ_b}{E} = \frac{a(1-3\mu)I}{2(1-\mu^2)} - \left[\frac{b^3+a^2 b}{s^3}\right]\frac{GJ_d}{E}$$

The five properties of the Traina solution are calculated depending on the properties of a plate element, E, G and I, and vary according to the torsional stiffness of the diagonal members of the grid-framework element. Thus, the torsional stiffness of the diagonal members is the dependent factor.

LIMIT ANALYSIS-MATRIX MODIFICATION

Elasto-plasticity is introduced into an elastic analysis with "plastic hinges" or actual hinges placed in the structure to prevent the addition of moment at that location. Hinge points occur where the structural bending moment is at the level of the plastic moment capacity of the grid-framework members and are inserted into the structure at the start of an analysis cycle.

The plastic moment capacity for a square grid framework element is determined by trial and error to be 0.293 times the element length times the moment of a fully yielded plate of unit width. This is verified by taking moment equilibrium of the interconnecting grid members at a fully yielded central node and dividing by the element length. The result, as expected, is the plastic moment per unit width of the plate being modelled. To date, this capacity is assumed valid for skewed and rectangular elements in lieu of an anticipated value of greater accuracy not yet known.

Installation of a hinge is a matter of the proper manipulation of Equations 2 prior to building the [S] matrix for a new analysis. For example, a hinge at i would result in zero moment at i or $F_i = 0$. The remaining bending moment F_j is written in terms of its corresponding displacement e_j. On the other hand, torsion modification cannot be so easily resolved. First, it is assumed that the torsional stiffness is subject to a reduction when the bending moment is at the plastic level. The ASCE Guide to Plastic Design (1971) provides a formula suitable to estimate the length of a plastic hinge for wide flange sections and a second formula to estimate the strain hardened shear modulus for steel. Both quantities are needed to generate the torsional stiffness by integrating over the two assumed distinct segments, elastic and plastic. Thus, the member stiffness matrix [S] is changed to reflect a hinge at i according to the new relationships for a typical member ij

$$F_i = 0$$

$$F_j = \frac{3EI}{L} e_j$$

$$F_k = \frac{GJG_{ST}}{L}\left[\frac{1}{\alpha_p G + (1 - \alpha_p)G_{ST}}\right] ek$$

where:

G_{ST} = strain hardened shear modulus

σ_p = torsional reduction factor

The torsional reduction factor is the ratio of the plastic hinge length to the grid member length and may be set to zero if no reduction in torsional stiffness is assumed. Similar modifications result for either a hinge at j or at both i and j.

LIMIT ANALYSIS-PROCEDURES

A grid-framework limit analysis is initiated with a solution to a plate structure by Equations 4 and 5 without matrix modification. The load proportion rather than magnitude is important and thus, the smallest load is normally taken to be unity with the remainder proportioned accordingly. A load factor of sufficient magnitude to cause at least one of the bending moments to attain a plastic moment level is determined. Moments and displacements are multiplied by the load factor. Hinges are inserted into the structure at the points where the moment has reached the plastic moment capacity.

A second cycle is initiated with a repeat analysis by Equations 4 and 5 but this time with appropriate "plastic hinge" matrix modifications. Again a load factor is found, moments and displacements adjusted, and hinge points identified to conclude the cycle. The analysis is continued for a number of cycles up to collapse of the structure. The cummulative load factor is the collapse load.

Two criteria are used to establish failure of the structure. Criteria one is a singular stiffness matrix with a zero inversion pivot indicating a structure with a sufficient number of hinges to cause instability. Criteria two is an excessive increase in displacement from one cycle to the next. Typically without collapse, the analytical cycles are terminated at twenty due to time restrictions.

EXAMPLE PROBLEM

The grid framework limit analysis was inserted into the bridge analysis computer program BRANDE IV (McCarthy, White, and Minor, 1980) to reduce the work requirements involved in this type of analysis. Subsequently, a number of plate structures were BRANDE IV elasto-plastically analyzed including the present example. STRUDL II (MIT, 1970) was used to check the elastic or first cycle solution and yield line theory (Woods and Jones, 1957) to check the ultimate behavior.

The example problem is the 54 element 70 node simply supported plate of Figure 5. The plate is steel with a modulus of elasticity $E = 30 \times 10^6$ psi, shear modulus $G = 12 \times 10^6$ psi, thickness $t = 2$ in., and Poisson's ratio $\mu = 0.25$. Loads are unit 1 kip magnitudes at each of the interior nodes to represent a uniform load over the plate. No reduction in torsional stiffness is assumed in a bending moment plastic hinge.

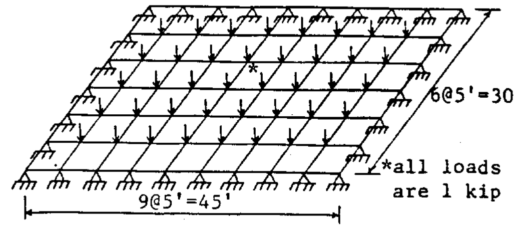

Fig. 5. Plate with a simulated uniform load.

An equivalent grid BRANDE IV limit analysis produced a twenty cycle load of 15.0 kips per internal node. A P-Δ plot of the node associated with maximum displacement, in Fig. 6, is consistent with curves of similar

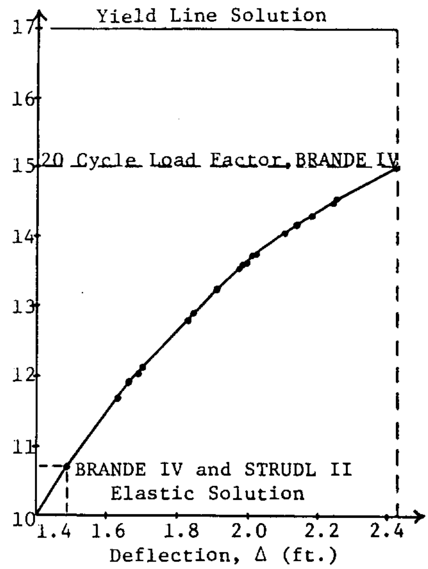

Fig. 6. Force-Displacement Curve.

type. An extrapolation of the curve indicates a collapse load that approaches the 18 kip level. A yield line analysis of the structure with a true uniform load produced a collapse load of 17 kips.

A comparison between the two techniques indicates a limit analysis collapse load that is approximately 6% above the yield line prediction. This is not unexpected for two reasons. First, the equivalent concentrated loads neglected the uniform load acting along the boundaries. Second, a nodal concentrated load is equal to the uniform load times the element area which necessarily neglects some of the distributed effect in much the same way as concentrated equivalents for a uniform beam load.

Having established that the ultimate load is consistent with the expected magnitude, the same consistancy must occur in the yield pattern to insure analytical confidence.

The yield line solution produced an overturned back-to-back Y yield pattern also revealed by the grid framework yield pattern of Fig. 7. There is scatter in the hinges but this is representative of true plate yielding. The hinge pattern progression started, as anticipated, toward the center of the plate moving generally outward to the corners.

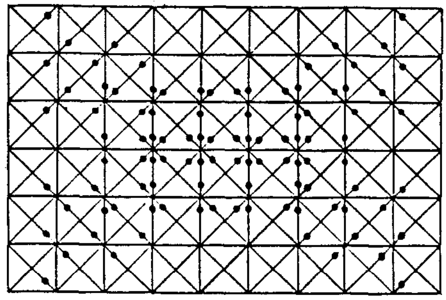

Fig. 7. Plastic hinge formation-twenty cycles.

CONCLUSIONS

A limit analysis by the grid framework method is a highly practical and proven approach. As with all new techniques, there are needed refinements like a concise definition of the plastic moment capacity for skewed and rectangular grids substantiated by further testing.

TABLE 1 The $\lfloor ASA^T \rfloor$ or Element Stiffness Matrix-Grid Framework

P \ X	1	2	3	4	5	6	7	8	9	10	11	12
1	EE+AB+AC+AD+AE	-AF+AG+AH-AI	AJ+AK	$\frac{AB-AC}{2}$	$\frac{-AF-AG}{2}$	-AJ	$\frac{AD-AE}{2}$	$\frac{AH+AI}{2}$	-AK	-EE	0	0
2	where:	AA+AL+AM+AH+AO	AP-AQ+AR	-AF-AG	$\frac{AL-AM}{2}$	AQ	$\frac{AH+AI}{2}$	$\frac{AN-AO}{2}$	-AR	0	$\frac{AA}{2}$	-AP
3			AS+AT+AU	AJ	-AQ	-AT	AK	AR	-AU	0	AP	-AS
4				EE+AB+AC+AV+AW	-AF+AG-AX+AY	-AJ-AZ	-EE	0	0	$\frac{AV-AW}{2}$	$\frac{-AX-AY}{2}$	AZ
5					AA+AL+AM+BC+BD	AP+AQ+BE	0	$\frac{AA}{2}$	-AP	$\frac{-AX-AY}{2}$	$\frac{BC-BD}{2}$	-BE
6						AS+AT+BF	0	AP	-AS	-AZ	BE	-BF
7							EE+AB+AC+AD+AE	-AF+AG-AH-AI	-AJ-AK	$\frac{AB-AC}{2}$	$\frac{-AF-AG}{2}$	AJ
8								AA+AL+AM+AN+AO	AQ-AP+AR	-AF-AG	$\frac{AL-AM}{2}$	-AQ
9									AS+AT+AU	-AJ	AQ	-AT
10										EE+AB+AC+AV+AW	AG-AF-AX+AY	AJ+AZ
11											AA+AL+AM+BC+BD	-AD-AQ-BE
12												AS+AT+BF

where:

$AA=\frac{4EI_a}{a}$ $AB=\frac{h^2BB}{b^2}$

$BB=\frac{4EI_b}{b}$ $AC=\frac{f^2FF}{b^2}$

$CC=\frac{4EI_c}{s_1}$ $AD=\frac{h^2CC}{s_1^2}$ $AI=\frac{hdGG}{s_1^2}$

$DD=\frac{4EI_d}{s_2}$ $AE=\frac{d^2GG}{s_1^2}$ $AJ=\frac{3hBB}{2b^2}$ $AN=\frac{d^2CC}{s_1^2}$ $AR=\frac{3dCC}{2s_1^2}$

$EE=\frac{GJ_a}{a}$ $AF=\frac{hfBB}{b^2}$ $AK=\frac{3hCC}{2s_1^2}$ $AO=\frac{h^2GG}{s_1^2}$ $AS=\frac{6AA}{2a^2}$ $AV=\frac{h^2DD}{s_2^2}$

$FF=\frac{GJ_b}{b}$ $AG=\frac{hfFF}{b^2}$ $AL=\frac{f^2BB}{b^2}$ $AP=\frac{3AA}{2a}$ $AT=\frac{6BB}{2b^2}$ $AW=\frac{g^2HH}{s_2^2}$ $AY=\frac{hgHH}{s_2^2}$ $BC=\frac{g^2DD}{2s_2^2}$

$GG=\frac{GJ_c}{s_1}$ $AH=\frac{hdCC}{s_1^2}$ $AM=\frac{h^2FF}{b^2}$ $AQ=\frac{3fBB}{2b^2}$ $AU=\frac{6CC}{2s_1^2}$ $AX=\frac{ghDD}{s_2^2}$ $AZ=\frac{3hDD}{2s_2^2}$ $BD=\frac{h^2HH}{s_2^2}$ $BE=\frac{3gDD}{2s_2^2}$

$HH=\frac{GJ_d}{s_2}$ $BF=\frac{6DD}{2s_2^2}$

TABLE 2 Force-Displacement Relationships-Plate Element

Case	P	1	2	3	4	5	6	7	8	9	10	11	12
Due to M_x	Force	$\frac{am_x}{2}$	0	0	$\frac{-aM_x}{2}$	0	0	$\frac{-aM_x}{2}$	0	0	$\frac{aM_x}{2}$	0	0
	Displ.	$\frac{bM_x}{2EI}$	$\frac{-\mu aM_x}{2EI}$	0	$\frac{-bM_x}{2EI}$	$\frac{-\mu aM_x}{2EI}$	0	$\frac{-bM_x}{2EI}$	$\frac{\mu aM_x}{2EI}$	0	$\frac{bM_x}{2EI}$	$\frac{\mu aM_x}{2EI}$	0
Due to M_y	Force	0	$\frac{bM_y}{2}$	0	0	$\frac{bM_y}{2}$	0	0	$\frac{-bM_y}{2}$	0	0	$\frac{-bM_y}{2}$	0
	Displ.	$\frac{-\mu bM_y}{2EI}$	$\frac{aM_y}{2EI}$	0	$\frac{\mu bM_y}{2EI}$	$\frac{aM_y}{2EI}$	0	$\frac{\mu bM_y}{2EI}$	$\frac{-aM_y}{2EI}$	0	$\frac{-\mu bM_y}{2EI}$	$\frac{-aM_y}{2EI}$	0
Due to M_{xy}	Force	$\frac{-bM_{xy}}{2}$	$\frac{-aM_{xy}}{2}$	0	$\frac{-bM_{xy}}{2}$	$\frac{aM_{xy}}{2}$	0	$\frac{bM_{xy}}{2}$	$\frac{aM_{xy}}{2}$	0	$\frac{bM_{xy}}{2}$	$\frac{-aM_{xy}}{2}$	0
	Displ.	$\frac{-2\Delta}{b}$	$\frac{-2\Delta}{a}$	Δ	$\frac{-2\Delta}{b}$	$\frac{-2\Delta}{b}$	$-\Delta$	$\frac{2\Delta}{b}$	$\frac{2\Delta}{a}$	Δ	$\frac{2\Delta}{a}$	$\frac{-2\Delta}{a}$	$-\Delta$

Limit analysis applications are varied and many. For the most immediate, overweight trucks are a consistent problem to the integrity of bridge structures. The reserve strength of bridges may be identified with a limit analysis. Those structures incapable of handling sustained overweight may be economically strengthened with the limit analysis plastic flow pattern as a guideline or simply be restricted in use.

REFERENCES

American Society of Civil Engineers (1971). Plastic Design in Steel-A Guide and Commentary, 2nd. Ed., ASCE-Manuals and Reports on Engineering Practice, No. 41, New York.

M.I.T. (1970). Department of Civil Engineering, ICES STRUDL II-Engineering User's Manual, 2nd Ed., Massachusetts Institute of Technology, Cambridge, Mass.

McCarthy, W.C. (1982). An Elastoplastic Plate Bending Finite Element With Applications to Bridge Structures, Final Report to the Engineering Foundation, New York.

McCarthy, W. C., K. White, and J. Minor (1982). BRANDE IV-A Bridge Analysis System, Proceedings of the 2nd Conference on Computing in Civil Engineering, ASCE, Baltimore, Maryland.

Traina, L. (1968). Matrix Analysis of Plate Structures in Bending, Doctorate Thesis, University of Wisconsin.

Wang, C. K. (1970). Matrix Methods of Structural Analysis, 2nd. Ed., International Textbook Company, Pennsylvania.

Wood, R. H., and L. L. Jones (1957). Yield Line Analysis of Slabs, American Elsevier Publishing Company, Inc., New York.

Yettram, A. L. and H. M. Husain (June 1965). "Grid-Framework Method for Plates in Flexure," Journal of the Engineering Mechanics Division, ASCE Proc., Vol. 91, June 1965, No. EM3.